Characterization of a Half-Apo Derivative of Peptidylglycine Monooxygenase. Insight into the Reactivity of Each Active Site Copper†

Shulamit Jaron and Ninian J. Blackburn*

Department of Biochemistry and Molecular Biology, Oregon Graduate Institute of Science and Technology, Beaverton, Oregon 97006-8921

Received December 15, 2000

ABSTRACT: A derivative of peptidylglycine monooxygenase which lacks the Cu_H center has been prepared and characterized. This form of the enzyme is termed the half-apo protein. Copper-to-protein stoichiometric measurements establish that the protein binds only one of the two copper centers (Cu_M and Cu_H) found in the native enzyme. Confirmation that the methionine-containing Cu_M has been retained has been obtained from EXAFS experiments which show that the characteristic signature of the Cu−S(Met) interaction is preserved. The half-apo derivative binds 1 equiv of CO per copper with an IR frequency of 2092 cm^{-1}, and this monocarbonyl also displays the Cu−S(Met) interaction in its EXAFS spectrum. These results allow unambiguous assignment of the 2092 cm^{-1} band as a Cu_M−CO species. Binding of CO in the presence of peptide substrate was also investigated. In the native enzyme, substrate induced binding of a second CO molecule with an IR frequency of 2062 cm^{-1}, tentatively assigned to a CO complex of the histidine-containing Cu_H site. Unexpectedly, this reactivity is also observed in the half-apo derivative, although the intensity distribution of the CO stretches now indicates that the copper has been partially transferred to a second site, believed to be Cu_H. The implications of this observation are discussed in terms of a possible additional peptide binding site close to the Cu_H center.

Copper monooxygenases use the reducing potential of copper to reversibly bind and activate oxygen for insertion into the C−H bond. They include the dicopper enzymes catechol oxidase, tyrosinase, dopamine β-monooxygenase (DβM),[1] peptidylglycine α-hydroxylating monooxygenase (PHM), and the more complex membrane-bound methane monooxygenase (pMMO). The first two enzymes are similar to the oxygen binding protein hemocyanin and possess binuclear copper active sites with short (2.9−4.6 Å) Cu−Cu distances and similar trishistidine ligation environments (*1*−*4*). The short metal distances allow the formation of bridging Cu−O_2−Cu species for reduction and utilization of dioxygen (*2*, *5*). DβM and PHM fall into a different subclass due to their longer Cu−Cu distance (11 Å) and inequivalent mononuclear copper sites (*6*, *7*). Both enzymes have similar active site structures and possess a Cu_M site, with two histidine ligands and one methionine ligand, and a Cu_H site, with three histidine ligands (*8*−*11*). PHM and DβM also appear to reduce oxygen in a similar manner, although the exact mechanism is still under investigation (*12*). A particularly intriguing question is how each copper is able to donate an electron to reduce dioxygen without forming a Cu−O_2−Cu bridging species.

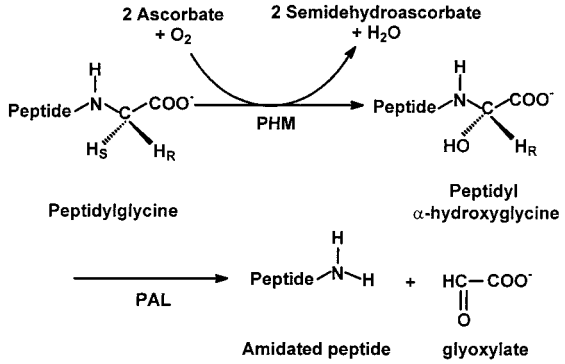

FIGURE 1: Overall reaction scheme of the bifunctional enzyme peptidylglycine α-amidase (PAM) broken down into its two constituent activities: peptidylglycine monooxygenase (PHM) and peptidyl α-hydroxyglycine lyase (PAL).

PHM catalyzes the hydroxylation of glycine-extended peptide hormones, the first step in the carboxy-terminal amidation of these messenger molecules (*13*−*15*). The overall mechanism is shown in Figure 1. Hydroxylation of substrates by PHM is dependent on ascorbate, molecular oxygen, and copper (*16*). The two active site copper atoms redox cycle through Cu(I) and Cu(II) forms, beginning in the resting state as Cu(II) (*17*). Ascorbate binds to the enzyme reducing the coppers, followed by the ordered binding of peptide substrate and then oxygen (*12*). Electrons are donated by each copper, reducing dioxygen to peroxide which is believed to be bound at the Cu_M site. The O−O bond is homolytically cleaved, and one atom of oxygen recombines at the glycine α-C atom of the peptide substrate forming the hydroxylated product and glyoxalate (*18*−*21*). Recent research has attempted to elucidate the method of electron

† This research was sponsored by Grant GM27583 from the National Institutes of Health (to N.J.B.).

* To whom correspondence should be addressed at the Oregon Graduate Institute, 20000 N.W. Walker Road, Beaverton, OR 97006-8921. Telephone: 503-748-1384. Fax: 503-748-1464. E-mail: ninian@bmb.ogi.edu.

[1] Abbreviations: DβM, dopamine β-monooxygenase; DW, Debye−Waller; d-YVG, dansyl-Tyr-Val-Gly; EXAFS, extended X-ray absorption fine structure; FT, Fourier transform; HPLC, high-pressure liquid chromatography; IR, infrared; PHM, peptidylglycine α-hydroxylating monooxygenase; XAS, X-ray absorption spectroscopy; YVG, *N*-acetyl-Tyr-Val-Gly.

10.1021/bi002849y CCC: $20.00
Published on Web 05/18/2001

donation by each copper. Crystal structures of PHM clearly show that the coppers are too far apart to form any type of bridging complex with dioxygen, and substrate turnover by the crystal has excluded the possibility of the coppers moving close together during turnover (*8*, *9*).

Two separate mechanisms have been proposed to explain how electron transfer might occur. The first mechanism is based on changes seen in the crystal structures of a variety of PHM adducts. Binding of substrate in these crystals creates a peptide bridge that significantly shortens the through-bond distance that the electron has to travel (*9*). Each copper plays a unique role in this mechanism, where Cu_M is the oxygen binding site, as historically assigned (*22*, *23*), and Cu_H is the electron donor. Although appealing, this mechanism has the major drawback that this type of outer-sphere reaction demands that there be very little reorganization of the copper ligands under redox conditions. However, we recently reported that major structural changes occur at both copper sites during reduction and oxidation (*11*). Large structural changes of this sort have a significant reorganizational energy barrier, which is likely to impede the electron transfer reaction. The second mechanism proposes that electron transfer takes place through the channeling of a superoxide molecule from one copper to the other (*24*). Reorganization of the copper ligands is not so problematic in this type of inner-sphere reaction, since ligand rearrangement during the oxidation of the copper centers might initiate the transfer of superoxide. While this mechanism is an interesting possibility, it too has major drawbacks; for example, superoxide may be more likely to diffuse away from the solvent accessible active site than to travel to the second copper.

The superoxide channeling mechanism was based on studies which suggested that both coppers might interact with dioxygen or oxygen intermediates during turnover. Infrared (IR) experiments revealed that there were two sites available for CO binding in the reduced enzyme: one that was activated by the reduction of copper with ascorbate and a second that was activated by the subsequent addition of peptide substrate. The IR frequencies associated with the two sites were 2092 and 2062 cm^{-1}, respectively, and were in the Cu−carbonyl stretching region (*25*, *26*). Earlier work on a half-apo derivative of the enzyme DβM definitively established the existence of a Cu_M−CO with a similar IR frequency of 2089 cm^{-1} (*22*, *27*, *28*). Assignment in PHM of 2092 cm^{-1} as a Cu_M−CO stretch was in part based on the findings from DβM, along with extended X-ray absorption fine structure (EXAFS) data of PHM−CO showing a lengthening of the Cu_M−S(Met) bond upon coordination of CO. Appearance of the second CO stretch at 2062 cm^{-1} was not accompanied by any change in the 2092 cm^{-1} stretch, ruling out the possibility of a second CO associated with Cu_M. Therefore, we proposed that CO binding at the Cu_H site caused the substrate-inducible IR frequency.

To establish the role of each copper in the reaction mechanism of PHM, it is necessary to individually characterize the chemistry at Cu_M and Cu_H. To this end, we have used previously developed methodologies to create a half-apo derivative of the native PHM (*22*). In this paper, we present our results on the selective removal of Cu_H from the active site of PHM and the subsequent characterization of Cu_M chemistry. The half-apo derivative confirms our original assignment of the Cu_M−CO infrared stretching frequency at 2092 cm^{-1} and provides evidence supporting the assignment of the 2062 cm^{-1} stretch as due to Cu_H−CO. Interestingly, binding of peptide substrate continues to activate the second CO infrared stretch at 2062 cm^{-1}, originally attributed to Cu_H−CO. We suggest that binding of substrate might actively participate in metal transfer between the copper sites, allowing CO binding at the Cu_H site. If this is the case, it may imply that there is a second peptide binding site close to the Cu_H site.

EXPERIMENTAL PROCEDURES

Purification of Native PHM. Native enzyme (PHMcc, catalytic core residues 42−356) was purified from a Chinese hamster ovary cell line overexpressing PHM. Complete details of the preparation of the cell line, cell growth, and enzyme isolation were previously published (*24*, *29*).

Determination of Copper and Protein Concentration. Protein concentration was calculated from the OD_{280} (1% w/w) = 0.98. Measurements were recorded on a Shimadzu UV-268 spectrophotometer at ambient temperature. Flame atomic absorption was used to determine copper concentrations in samples. Measurements were made on a Varian-Techtron AA5 spectrometer.

Synthesis of the Half-Apo PHM Derivative. Samples of native PHM were selected that were known to have a copper-to-protein ratio of 2:1, activities in the normal range, and which showed normal spectroscopy. An aliquot (500 μL) of the enzyme was dialyzed in 800 mL of buffer (50 mM potassium phosphate, pH 7.5) on ice with stirring. Carbon monoxide was then bubbled through the buffer for at least 8 h. Once the buffer and the sample were equilibrated with CO, an excess (at least 5 equiv per Cu) of anaerobic ascorbate (stock, 330 mM in MES, pH 5) was added directly to the dialysis bag in an anaerobic environment. The dialysis bag was returned to the buffer, and bubbling with CO was continued for at least another 8 h. This procedure left the enzyme in the dialysis bag reduced and carbonylated, while excess ascorbate was dialyzed away. An aqueous stock solution of 0.1 M NaCN/0.2 M NaCl was bubbled with argon until anaerobic. Enough of this solution was transferred anaerobically to the dialysis buffer to produce a 10 μM final cyanide concentration. Again, CO was bubbled through the buffer for at least 8 h to allow cyanide equilibrium across the dialysis membrane while maintaining the [CO] at saturating levels. Cyanide is able to bind to Cu(I) centers with vacant coordination sites and eventually will strip the metal out of the protein. Theoretically, carbon monoxide should protect the Cu(I) center from cyanide attack by effectively competing with CN^- for the vacant coordination position. Following cyanide equilibration, the dialysis tubing containing the treated enzyme sample was transferred under anaerobic conditions to fresh, CO-saturated, anaerobic potassium phosphate buffer (50 mM, pH 7.5), free of cyanide. This again was allowed to equilibrate for at least 8 h with CO bubbling, and the previous step was repeated to allow complete removal of copper−cyanide complexes and any free cyanide. The sample was then transferred to a conical vial under anaerobic conditions and left under 1 atm of CO. Samples were removed for copper analysis, CO stoichiometry, infrared spectroscopy, high-pressure liquid chromatography (HPLC) analysis, and X-ray absorption spectroscopy (XAS).

Measurement of CO Stoichiometry. The half-apo sample, created by the previous method, produces a carbonylated enzyme. A sample of the half-apo enzyme (10 μL) and a sample of the CO-saturated dialysis buffer were each transferred to separate conical vials. The dialysis buffer was used to determine the background CO concentration. An equal pressure (~1 atm) of CO was introduced to both samples in tandem. The concentration of carbon monoxide in each sample was measured as previously described (*24*).

Infrared Spectroscopy of Protein Samples. IR spectroscopy was carried out on a Perkin-Elmer System 2000 FTIR with a liquid nitrogen-cooled mercury cadmium telluride detector. Samples of enzyme solutions (50 μL) were injected into a 0.050 cm path-length sample cell with CaF_2 windows. The cell was placed in a constant humidity chamber and kept at 10 °C to control the outgassing of carbon monoxide in the solution. Two hundred scans of each sample were collected and averaged using Spectrum for Windows (Perkin-Elmer). Interference from the large water absorption at 2140 cm^{-1} was eliminated by subtraction of a water spectrum. Simulation of the IR data to determine the peak frequency and area was performed on Grams/386 version 3.04 (Galactic Industries Corp.).

XAS Data Collection and Analysis. XAS data were collected at the Stanford Synchrotron Radiation Laboratory (SSRL) on beam lines 7.3 (BL 7.3) and 9.3 (BL 9.3) operating at 3.0 GeV with beam currents between 100 and 50 mA. An Si220 monochromator with 1.2 mm slits was used to provide monochromatic radiation in the 8.8−10 keV energy range. Harmonic rejection was achieved either by detuning the monochromator 50% at the end of the scan (9731 eV, BL 7.3) or by means of a rhodium-coated mirror with a cutoff of 13 keV placed upstream of the monochromator (BL 9.3). The protein samples were measured as frozen glasses in 20−30% ethylene glycol at 11−14 K in fluorescence mode using either a 13-element (BL 7.3) or 30-element (BL 9.3) Ge detector. To avoid detector saturation, the count rate of each detector channel was kept below 110 kHz, while the rise in fluorescent counts through the edge was kept below 20 kHz per channel. Under these conditions, no dead-time correction was necessary. A Soller slit assembly fitted with a 6 μ Ni filter was used in conjunction with the 30-element detector of BL 9.3 to decrease the elastic scatter peak and further reduce detector saturation. The summed data for each detector channel were then inspected, and only those channels that gave high-quality backgrounds free from glitches, drop outs, or scatter peaks were included in the final average. Data analysis was performed as previously described (*11*, *30*). The parameters refined in the fit were as follows: E_0, the photoelectron energy threshold; R_i, the distance from Cu to atom i; and $2\sigma^2_i$, the Debye−Waller (DW) term for atom i. Multiple scattering contributions were included for CO and imidazole ligands. Imidazole rings were simulated as rigid groups with fixed internal ring geometry, such that the imidazole outer shell distances were defined by the Cu−N(imid) distance and the orientation of the ring to the Cu−N bond axis. The orientation was initially chosen to be symmetrical, with the ring plane coincident with the Cu−N axis, but Cu−Cβ and Cu−Cγ/Nγ distances were later allowed to vary by up to 5% of their idealized values during refinement. The coordination numbers were also allowed to vary but were constrained to produce DW factors within reasonable limits (first shell, $0 < 2\sigma^2 < 0.015$; $\sigma^2_{\text{second shell}} \geq \sigma^2_{\text{first shell}}$). The goodness of fit was judged by reference to a goodness of fit parameter, F, defined as

$$F_2 = \frac{1}{N}\sum_{i=1}^{n} k^6(\text{data}_i - \text{model}_i)^2$$

(Tables S1−S7, Supporting Information.)

Activity Measurements and Substrate Turnover. HPLC was used to measure production of the hydroxylated product by the half-apo derivative. Oxygen consumption by a particular enzyme sample was first measured on a Strathkelvin Instruments 1302 oxygen electrode connected to a model 781 oxygen meter. Samples were kept at 37 °C by water circulation in a RC300 respiration cell, and a magnetic spin-bar was placed in the chamber for continuous stirring. Various reaction mixtures were created, and the volume was equilibrated to 2000 μL by addition of MES (100 mM, pH 5.5). All reactions were steady state and were left open to air. Final concentrations in the mixture were 0.1 μM PHM, 250 μM *N*-acetyl-Tyr-Val-Gly (YVG) or dansyl-Tyr-Val-Gly (d-YVG), 1.5 mM ascorbate, 0.01 mg/mL catalase, and 5 μM Cu^{2+}. Reaction mixtures analyzed were (1) half-apo, d-YVG, (2) half-apo, d-YVG, ascorbate, (3) half-apo, d-YVG, Cu, and (4) half-apo, d-YVG, Cu, ascorbate. All reaction mixtures were allowed to equilibrate without d-YVG, and activity was initiated by the addition of peptide substrate. Oxygen consumption was measured for 2 min, and after 10 min of reaction time, each mixture was quenched with 200 μL of TFA (0.1% in water). The samples were then passed through a 10 000 molecular weight cutoff membrane to remove large protein. The filtrate was injected onto a Waters Delta PAK column (5 μm C18 100A, 3.9 × 150 mm), controlled by a Waters 501 HPLC pump, in solvent A (0.1% TFA in water), and the following solvent profile was used to separate peptides: 5 min with solvent A, 5 min gradient to a mixture of 50% solvent A and 50% solvent B (0.1% TFA in 80% acetonitrile), 5 min at this mixture, 5 min gradient to 100% solvent B, 5 min at 100% solvent B, 5 min gradient to 100% solvent A, and 10 min in 100% solvent A. Effluent was measured on a Waters 474 fluorescence detector set to an excitation $\lambda = 340$ nm and an emission $\lambda = 557$ nm. Retention times for d-YVG and its hydroxylated product (d-YVG-OH) were around 16 and 15.5 min, respectively.

RESULTS

Stoichiometry of Copper Binding to Half-Apo PHM. A fresh preparation of the fully metalated PHM (two coppers) was carbonylated in the normal way. This strategy was previously shown to produce an enzyme with one CO per two coppers (*24*). Dialysis of the preparation with cyanide is expected to strip any copper from the enzyme that is not protected by the binding of CO. Following removal of excess cyanide, $Cu(CN)_x^{(x-1)-}$ complexes, and free copper by repeated dialysis with fresh buffer, the copper-to-protein ratio of PHM dropped to 0.97 (Table 1, average of eight independent determinations). At the chosen [CN^-], the final Cu-to-PHM ratio was independent of the length of dialysis.

Oxygen Activity and Turnover by Half-Apo PHM. Oxygen consumption by the half-apo derivative was measured on

Table 1: Copper-to-Protein Stoichiometry of Eight Individual Preparations of Half-Apo PHM and Their Average

prepn	XAS no.	[Cu]	[protein]	Cu:protein
1		0.454	0.557	0.815
2	S200	1.000	0.875	1.143
3		0.540	0.627	0.861
4	9300	0.465	0.420	1.107
5	9500	0.371	0.428	0.867
6		3.735	3.700	1.009
7	S1199	0.582	0.504	1.155
8		0.224	0.283	0.792
av				0.969

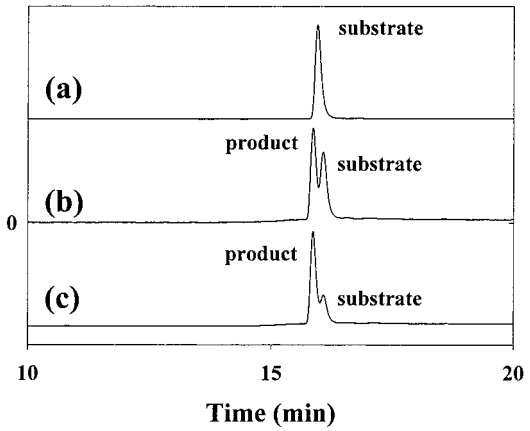

FIGURE 2: HPLC separation of the dansylated substrate d-YVG from product d-YVG-OH following PHM turnover: (a) half-apo + catalase + Cu + d-YVG; (b) half-apo + catalase + ascorbate + d-YVG; (c) half-apo + catalase + Cu + ascorbate + d-YVG.

an oxygen electrode. The specific activity of half-apo PHM without additional copper (d-YVG substrate) was 2.5 μmol of $O_2 \cdot mg^{-1} \cdot min^{-1}$. The addition of excess copper to the enzyme increased the specific activity to 3.4 $\mu mol \cdot mg^{-1} \cdot min^{-1}$. The activity of a fully metalated native control was 5.9 $\mu mol \cdot mg^{-1} \cdot min^{-1}$. The specific activity is diminished in the half-apo derivative, even upon the addition of exogenous copper, and indicates that some PHM functionality is probably lost by the derivatization by cyanide dialysis. The ability of half-apo PHM to hydroxylate its peptide substrate was measured via HPLC (Figure 2, peaks have been normalized). Loss of one copper site in half-apo PHM might be expected to abolish turnover of the enzyme. Addition of excess copper to the enzyme without ascorbate results in zero oxygen consumption and no product formation (Figure 2a). However, when ascorbate is added, in either the presence or absence of copper, the enzyme begins to react with oxygen and product is formed. Without added copper, oxygen consumption is slow, and there is only 50% turnover of substrate within 5 min (Figure 2b). When excess copper is added to the reaction, the oxygen activity increases, and within 5 min 80% of substrate has been converted to product. Clearly, loss of the second copper site affects the overall ability of the half-apo enzyme to turn over substrate, although the enzyme is still partially active. Because the copper in oxidized PHM is labile, intermolecular copper transfer is possible, and this process can be accelerated by redox cycling. Thus, under steady-state conditions, roughly one-fourth of the molecules present might be fully metalated at any given time. Fully metalated molecules of PHM are likely to retain catalytic activity, thus explaining how a sample of half-apo might retain some activity. Alternatively, some reconstitution may occur from trace concentrations of cupric ions adsorbed to surfaces or present in reagents. Previous studies with apo DβM showed that it is almost impossible to prevent low levels of reconstitution of the enzyme from these trace sources of copper (*31*).

EXAFS Spectroscopy of Half-Apo PHM and Half-Apo PHM in the Presence of Bound YVG Substrate. The structural environment of the coppers in half-apo PHM was probed using EXAFS. All samples were previously determined to bind a single equivalent of copper. To produce a sample of half-apo PHM without bound CO, the carbonylated half-apo derivative was exposed to three cycles of vacuum flushing with argon. The EXAFS and Fourier transform (FT, $\Delta k = k_{min}$ to k_{max}) of a typical half-apo sample (S1199, Tables 1 and 2) are shown in Figure 3a (S1199 fit A, Table 2). The two resolved first shell peaks were fit [distance R (Å), DW (Å^2)] with 2 N(His) at 1.96 (0.006) Å and 1 S(Met) at 2.31 (0.018) Å. Although the first shell distances are similar in half-apo and reduced native PHM, the splitting of the first shell Cu−N and Cu−S is more pronounced. To test the relationship to the native structure, the DW of the sulfur atom in the half-apo EXAFS was set to the value found in native PHM (*11*), and the coordination number and distance for this atom were refined. If, as anticipated, the enzyme contains only the Cu_M site, an increase in intensity of the sulfur shell in the EXAFS is expected, due to an increase in the average sulfur component from 0.5 S in native PHM to 1 S in the half-apo enzyme. With the DW fixed at 0.013 Å^2 (the value found previously for native reduced enzyme) the S coordination number rises from 0.5 to 0.9. This is fully consistent with the formulation of the half-apo derivative as having a single Cu_M center and no Cu_H. Figure 3b shows the best fit obtained when the S(Met) contribution is eliminated. The high R shoulder on the first shell in the FT is not fit, the EXAFS fit becomes much poorer, and F more than doubles to 1.22. The results of curve fitting the EXAFS of four separate preparations of the half-apo enzyme are given in Table 2. The average Cu−N(His) and Cu−S(Met) distances and their DWs derived from these fits are 1.97 (0.007) Å and 2.28 Å (0.019), respectively.

Figure 4 shows the experimental and simulated EXAFS of the half-apo enzyme treated with the peptide substrate YVG. Binding of the YVG substrate appears to have a significant effect on the XAS, which is most apparent in the FT. Simulation of the data indicated that fits employing a single shell of Cu(I)−imidazole interactions (2 imid at 1.93 Å, 1 S(Met) at 2.27 Å, $F = 0.78$) did not reproduce well the FT shells at 2.3 and 2.8 Å (S200 fit A, Table 2). On the other hand, fits which entertained the possibility of partial (∼50%) copper migration to the H site were significantly better. Thus, splitting the imidazole shell into two (0.9 Cu−imid at 1.98 Å and 1.1 Cu−imid at 1.87 Å), together with a decreased intensity S(Met) interaction (0.5 S at 2.26 Å), provided a much improved fit, since the outer shell contributions from the shorter imidazole shell now fit well to the 2.8 Å transform feature. The split imidazole shell fit produced an 81% decrease in the F value to 0.43 (S200 fit B, Table 2) and was reminiscent of fits obtained for the fully metalated reduced enzyme, where the Cu_M and Cu_H centers were found to have significantly different Cu−N(imid) bond lengths of 1.98 and 1.88 Å, respectively. An additional feature of the fit (Table 2) was the need to include an additional shell of

Table 2: First Shell EXAFS Fitting Parameters for a Number of Different Preparations of Half-Apo PHM and Their Derivatives with Bound Substrate and CO[a]

	N(His)			S(Met)			C(CO)			
sample	*N*	distance	DW	*N*	distance	DW	*N*	distance	DW	*F*
half-apo										
S1199 fit A	2	1.96	0.004	1	2.31	0.018				0.570
S1199 fit B	2	1.97	0.006	0						1.220
S200	2	1.94	0.007	1	2.27	0.019				1.006
9300	2	1.96	0.007	1	2.30	0.016				0.855
9500	2	2.00	0.010	1	2.25	0.022				1.025
half-apo−YVG										
S200 fit A	2	1.92	0.010	1	2.27	0.019				0.784
S200 fit B	0.9	1.98	0.007	0.5	2.26	0.008				0.430
	1.1	1.87	0.003							
half-apo−CO										
9300	2	1.97	0.005	1	2.28	0.019	1	1.82	0.001	0.699
9500	2	1.96	0.009	1	2.25	0.016	1	1.79	0.008	0.492

[a] Distances are quoted in Å and DW factors in Å^2. Errors in coordination numbers are approximately 25% while errors in distances are ±0.02−0.03 Å. *F* refers to the goodness of fit parameter defined in the text. Sample identity is defined in Table 1.

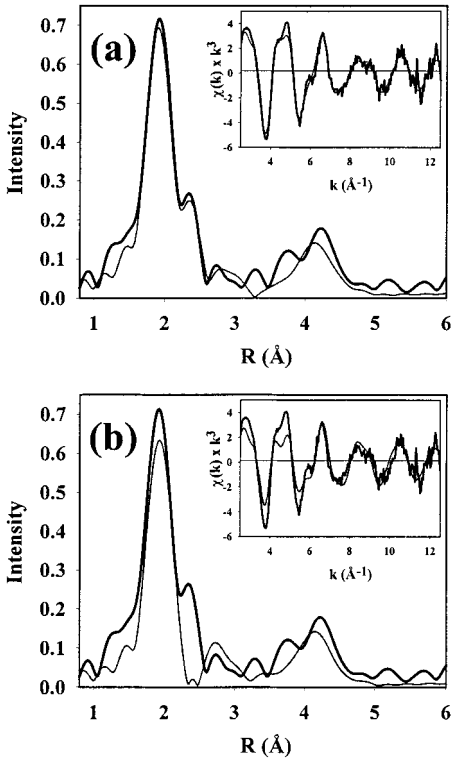

FIGURE 3: Experimental and simulated FT and EXAFS (inset) for the sample S1199 of half-apo PHM: (a) simulated with a contribution from 1 S(Met) scatterer; (b) simulated without any contribution from the S(Met) scatterer. Raw data are shown with thick lines and simulated data with thin lines. Parameters used to fit the data are shown in Table 2.

low Z scatterers (0.5 N/O at 2.55 Å), without which the breadth of the transform in the 2.2−2.8 Å range could not be reproduced. The extra O/N shell may be derived either from an ordered water molecule or from the third histidine ligand at the H site (H172), which is only weakly coordinated to the copper (*11*). Consistent with the 50% decrease in Cu−S(Met) occupation number, the data therefore suggest that binding of substrate to the half-apo enzyme induces migration of copper from Cu_M to Cu_H.

Stoichiometry of CO Binding to Copper in Half-Apo PHM. Following the construction of half-apo PHM, the enzyme was left under 1 atm of carbon monoxide gas. The concentration of half-apo-bound CO was determined by a titration

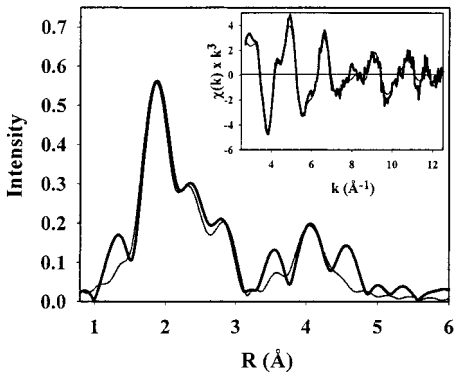

FIGURE 4: Experimental and simulated FT and EXAFS (inset) for the sample S200 of half-apo PHM treated with 2 equiv per Cu of peptide substrate YVG. Raw data are shown with thick lines and simulated data with thin lines. Parameters used to fit the data are shown in Table 2.

Table 3: Stoichiometry of CO Binding to Five Individual Preparations of Half-Apo PHM and Their Average

prepn	[CO]	[Cu]	CO:Cu
1	0.521	0.454	1.148
2	0.751	0.599	1.254
3	0.611	1.095	0.558
4	0.702	0.469	1.497
5	0.370	0.340	1.088
av			1.109

of PHM into hemoglobin (previously described in ref *24*). Five different preparations and their average are shown in Table 3. An average ratio of 1.1 CO per copper was determined, which indicated that all of the copper atoms bound to the half-apo protein also bind CO.

Infrared Spectroscopy of Half-Apo PHM−CO. Following the assessment of copper and carbon monoxide content, samples of the half-apo enzyme were taken for infrared analysis. All samples analyzed were known to bind a single atom of copper and a single molecule of carbon monoxide. The infrared spectrum of the Cu−C≡O stretching region of a typical half-apo−CO sample is depicted in Figure 5a and shows a single, strong absorption peak at 2092 cm^{-1}. Confirmation of this band as a Cu−CO and not inorganic $Cu(CN)_3^{2-}$, the IR frequency of which is found at 2094 cm^{-1} (*25*), comes from substitution with isotopically labeled ^{13}CO, which shows a shift of the CO stretch to 2044 cm^{-1}

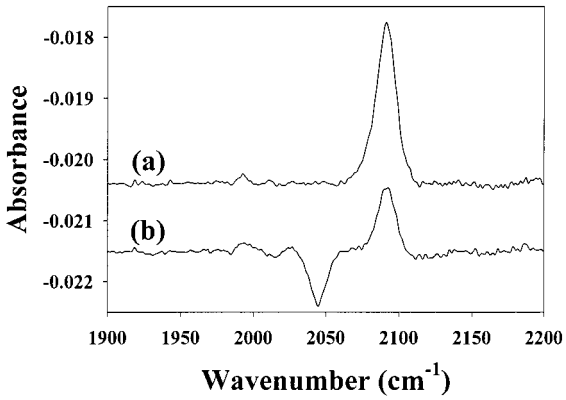

FIGURE 5: Infrared spectra of the carbonylated half-apo enzyme: (a) half-apo PHM + ^{12}CO; (b) ^{12}CO minus ^{13}CO data.

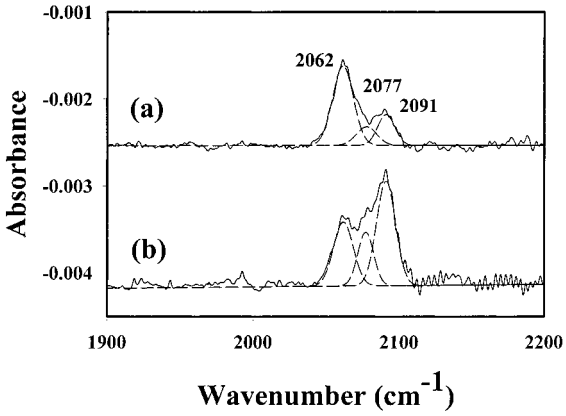

FIGURE 6: Infrared spectrum of the carbonylated half-apo enzyme with bound YVG: (a) half-apo PHM exposed to CO and then treated with 2 equiv of YVG; (b) half-apo PHM treated with 2 equiv of YVG and then exposed to CO. Gaussian curve fitting of the IR peaks is included as dotted lines below the curves.

(Figure 5b). Additionally, vacuum flushing of the carbonylated sample with argon leads to a loss of the 2092 cm^{-1} intraligand-stretching band, indicating that this stretch derives from a dissociable gaseous molecule, namely, CO. Because there is only one CO bound per Cu, all of the copper remaining bound in half-apo PHM binds carbon monoxide with a stretching frequency of 2092 cm^{-1} and therefore must have the same ligand environment. An identical C≡O stretching frequency was identified in native PHM (*23*, *24*).

Infrared Spectroscopy of PHM−YVG−CO. Addition of the YVG substrate to half-apo PHM, before or after the addition of CO, causes the appearance of a second CO stretching frequency at 2062 cm^{-1} (Figure 6), similar to what was seen in native PHM. The integrated intensity of both the 2092 and 2062 cm^{-1} peaks remains approximately equal to that of the 2092 cm^{-1} single peak in the absence of substrate. However, the relative intensities of 2092 and 2062 cm^{-1} bands depend on the order of substrate addition. When CO is bound first (Figure 6a), the 2062 cm^{-1} peak dominates the spectrum; when YVG is bound first (Figure 6b), the 2092 cm^{-1} peak dominates. Additionally, a third peak is detected by Gaussian fitting at 2077 cm^{-1} in both cases, which is unique to the half-apo species. In an experiment using ^{13}CO gas, the 2092 and 2062 cm^{-1} bands were observed to red shift by 46−50 cm^{-1}, proving their identity as Cu−CO species; but in this case, no third band could be detected (data of low signal-to-noise ratio not shown). In native PHM,

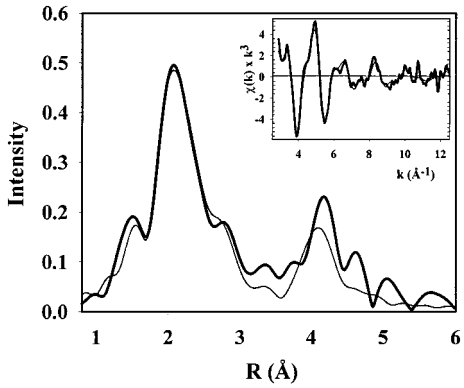

FIGURE 7: Experimental and simulated FT and EXAFS (inset) for the sample 9500 of half-apo PHM−CO. Raw data are shown with thick lines and simulated data with thin lines. Parameters used to fit the data are shown in Table 2.

binding of YVG was observed to activate CO binding at a second site (2062 cm^{-1}) regardless of order of substrate/CO addition and without a loss of intensity at 2092 cm^{-1}. The substrate-activated CO binding site in that enzyme was hypothesized to be at Cu_H because of an increase in the CO-to-Cu ratio from 0.5 to 1.0 that did not cause a shift in the 2092 cm^{-1} Cu_M−CO.

EXAFS Spectroscopy of Half-Apo PHM−CO. EXAFS and FT data for a sample of the half-apo−CO complex (sample 9500, Tables 1 and 2) are shown in Figure 7. Simulations included the O atom of the C−O group (at the appropriate distance for a linear Cu−carbonyl) with its associated multiple scattering. The three different first shell ligands are clearly defined in the FT, 2 N(His) at 1.96 Å, 1 S(Met) at 2.25 Å, and a short Cu−C(CO) at 1.79 Å. One noticeable difference in the half-apo−CO structure is that the Cu−S distance remains unchanged from half-apo within experimental error. In native reduced PHM, there was a 0.08−0.10 Å lengthening of the Cu−S distance upon carbonylation of the enzyme (*24*). Regardless of the differences in ΔR_{Cu-S}, these data indicate that in half-apo PHM the copper and the CO are both bound at the Cu_M site. Fits for two independent samples of half-apo PHM−CO are given in Table 2.

DISCUSSION

Characterization of the Half-Apo Cu_M−Carbonyl Complex. Determining the reactivity of each copper is crucial to understanding the mechanism of electron transfer in PHM, and information of this sort may aid in distinguishing between the conflicting mechanisms. One way to investigate each copper individually is to create PHM derivatives where a single copper is present. In this paper, we describe the successful preparation of a half-apo derivative containing only the Cu_M site and its subsequent characterization.

Cyanide is known to compete with oxygen for the Cu(I) binding sites in proteins such as DβM (*22*, *32*, *33*) and hemocyanin (*34*, *35*) due to its propensity to both coordinate and remove copper from the proteins. Results from the cyanide dialysis of native PHM show that demetalated derivatives can likewise be formed in this enzyme. Previous studies suggested that binding of CO initially takes place at only one copper center (*23*, *24*, *27*, *28*). By occupying one coordination site with CO, the copper is protected from binding of additional ligands while the other copper is

susceptible to stripping from the protein by cyanide in solution. Indeed, cyanide dialysis is able to remove the nonprotected copper center in PHM, leaving a half-apo derivative (copper-to-protein stoichiometry of 1:1). Furthermore, this manipulation does not adversely affect the enzyme's ability to hydroxylate substrate, because the addition of excess copper restores a significant fraction of native activity.

Carbonylation of the half-apo derivative produces a Cu−CO with a single IR stretching frequency of 2092 cm^{-1} and a 1:1 CO-to-Cu ratio. Previous investigations of the native PHM assigned the 2092 cm^{-1} IR frequency as a Cu_M−carbonyl. Since the structure of the copper center in half-apo PHM shows a strong Cu−S interaction derived from Met 314 in both the reduced and carbonylated forms, the half-apo enzyme must contain only the Cu_M center, providing unambiguous assignment of the 2092 cm^{-1} band as a Cu_M−monocarbonyl.

The 2.28 Å Cu−S(Met) bond is 0.04 Å longer than the distance in the reduced native enzyme (2.24 Å), suggesting that removal of Cu_H causes a small perturbation at the Cu_M site. Carbonylation of native PHM caused a 0.1 Å lengthening of this bond to 2.34 Å due to the coordination of a fourth ligand at the Cu_M site. EXAFS data indicate that while binding of the peptide substrate to the half-apo protein produces little change in the XAS-derived metrical parameters for the Cu_M center, it does appear to induce migration of copper from the M site to the H site. Consistent with this finding, IR evidence establishes that peptide binding activates an additional CO binding site (probably at Cu_H) in a fashion similar to what is observed in native reduced PHM (*11*). On the basis of this, we would reason that binding of peptide appears to increase the affinity of the H site for Cu(I). However, crystallographic results of substrate binding to oxidized PHM show substrate binding close to the Cu_M, requiring the active site residues Asn 316, Tyr 318, and Arg 240 to form hydrogen bonds to the peptide backbone of the substrate (*9*). Two of these residues, Asn 316 and Tyr 318, are located on the same β-strand as Met 314, and perturbation by the binding of substrate would be expected to affect the position of Met 314 in relation to Cu_M. Indeed, the K_m for YVG was significantly increased in the M314I mutant (*36*). Since there are no major changes in the Cu_M ligand environment in either the half-apo enzyme or native PHM when substrate is bound, we suggest that there might be a second stable substrate binding site as yet undetected by crystallography. We have observed that the substrate-activated C≡O stretching frequency (2062 cm^{-1} for YVG) is dependent upon the specific substrate bound [benzoylglycine, 2075 cm^{-1} (*24*); DL-benzoylalanine, 2070 cm^{-1} (unpublished)], while the 2092 cm^{-1} Cu_M−CO frequency is not. This would lead us to conclude that substrate binding is taking place close to a second site of CO binding that is somewhat distant from Cu_M. It is possible that during catalysis, peptide substrate is mobile, but when one or more components needed for turnover are limiting, an intermediate can be trapped. The observed intermediate might be unique, depending on the experimental method (i.e., pH and temperature), explaining why crystallography and EXAFS show conflicting results for substrate binding. If more than one substrate binding site is important in the mechanism of PHM, it is possible that during catalysis substrate switches between the two sites, perhaps initiated by the oxidation of one copper and facilitating electron transfer.

In the related enzyme DβM, a chemically derived half-apo DβM was created which also selectively removed the Cu_A (Cu_H in PHM) site (*22*). An infrared frequency of 2089 cm^{-1} from the carbon monoxide adduct of half-apo DβM was assigned to CO binding at the Cu_M center, which is similar to that described here for half-apo PHM. Nonetheless, the EXAFS of the half-apo DβM differs significantly from that of half-apo PHM. For both enzymes, an increase in the average sulfur component from 0.5 S per Cu in fully metalated protein to 1.0 S per Cu in half-apo protein is expected to increase the intensity and/or decrease the DW term of the sulfur shell in the FT. Half-apo DβM indeed follows this rule, with a significant decrease in the DW from 0.015 $Å^2$ in the reduced enzyme to 0.006 $Å^2$ in the half-apo enzyme (*10*, *22*). In the PHM case, although the intensity of the S shell doubles in half-apo as expected, the DW is large (0.017 $Å^2$) for a single Cu−S(Met) interaction. Large DW terms generally indicate either a spread in metal−ligand distance or partial site occupancy. We have already determined that the copper in half-apo PHM all resides in the same chemical environment; therefore, it is likely that the large DW term for the Cu−S bond in half-apo PHM is due to a spread in the Cu−S distances. Reduced native PHM was also found to have a Cu−S DW (0.013 $Å^2$) that was unusually large for a unique Cu−S bond, whereas in the native CO adduct the DW decreased and the Cu−S interaction became much better defined. This decrease in DW in half-apo−CO is not observed. These anomalous DW terms imply that a variety of configurations exist with differing Cu−S interactions, suggesting the existence of "methionine-on" and "methionine-off" conformers. The movement of the Met ligated to Cu_M thus appears to be coupled in some way to the occupancy [and/or oxidation state (*11*)] of the Cu_H center and may indicate a significant role for this ligand in the mechanism of oxygen activation and/or electron transfer. How these ligand dynamics are involved and what trigger initiates the changes are still unclear.

Changes in the Active Site Caused by Substrate Binding. Cu_M has been unambiguously identified as the sole copper site in the active site of half-apo PHM, and this has helped to confirm the assignment of the Cu_M−CO infrared frequency as 2092 cm^{-1}. In our earlier work, we identified a second CO binding site in native PHM that was activated by peptide substrate binding and showed an IR frequency of 2062 cm^{-1} (*24*). We proposed that this CO vibration was a copper−carbonyl caused by CO binding at the Cu_H site. In half-apo, binding of substrate was therefore not expected to induce binding of CO at any additional sites or significantly perturb the Cu_M−CO already bound. Surprisingly, when substrate was bound to half-apo PHM, there was a significant decrease in the Cu_M−CO IR intensity (2092 cm^{-1}) along with the appearance of two new peaks at 2077 and 2062 cm^{-1}.

The 2077 cm^{-1} stretch is most likely caused by small quantities of the copper−cyanide complex $[Cu(CN)_4]^{3-}$ remaining in solution, which becomes detectable due to the low intensity of the 2092 and 2062 cm^{-1} Cu−CO stretches. However, the presence of the second CO binding site with a 2062 cm^{-1} frequency is unanticipated in an enzyme thought to lack all but a single copper site. There appear to be two possible explanations for this IR frequency that fit with our

previous data. First, substrate binding in the vicinity of Cu_M in half-apo PHM might "super" activate the copper to ligate two or more molecules of carbon monoxide, or, second, substrate binding in half-apo might cause transfer of copper to the Cu_H site where it is activated to bind copper. Indeed, the EXAFS simulations described above have provided evidence that the latter may indeed occur.

The first hypothesis, suggesting that Cu_M binds additional molecules of CO, is appealing because half-apo PHM contains only a Cu_M site, which is thought to be a site of oxygen activity in the native enzyme. However, the copper−carbonyl stretching frequency should shift to higher frequency with ligation of additional CO groups. Studies on the coordination of CO to osmium compounds [$OsHCl(CO)(PPh_3)_2$ and $OsH_2(CO)_2(PPh_3)_2$] emphasize this point. The monocarbonyl−Os complex exhibits one IR detectable frequency: the asymmetric stretch at 1912 cm^{-1}. Coordination of a second molecule of CO to form the bis complex induces a second IR frequency, a bending mode, at 2014 cm^{-1} and causes a shift to higher frequency (1990 cm^{-1}) of the asymmetric stretching mode (*25*). The fact that there is no upward shift in the Cu_M 2092 cm^{-1} frequency suggests that the Cu_M site is not involved in the substrate-activated CO binding site. A further argument against the biscarbonyl assignment for the 2092 cm^{-1} band can be made on the basis of the expected decrease in π-back-bonding. As the number of bound CO molecules increases, the extent of back-bonding to each CO should diminish with an associated increase in υ(CO) rather than the decrease in frequency to 2062 cm^{-1}, which is observed experimentally. Thus, it appears very unlikely that the 2062 cm^{-1} IR frequency seen in half-apo PHM is due to CO binding as $Cu_M(CO)_2$.

The second explanation for the appearance of a stretch at 2062 cm^{-1} is that binding of substrate induces movement of the copper from the Cu_M site into the Cu_H site. We have argued in a previous paper that the peptide-induced CO stretch in native PHM falls into the range of trishistidine-ligated coppers and is therefore consistent with CO binding at the three histidine-ligated Cu_H site (*24*). Model compounds of trisimidazole−Cu complexes with bound CO are reported to have a υ(CO) at 2080 cm^{-1} (*37*) at the high end, while CO complexes in hemocyanins are found between 2043 and 2063 cm^{-1} (*38*). Substrate binding in half-apo PHM appears to induce CO binding at a site similar to the trishistidine models. The empty Cu_H center in half-apo clearly fits this description, and the IR spectra of native PHM−CO with bound substrate which showed the same C≡O stretch at 2062 cm^{-1} was assigned as CO binding to the Cu_H site. If this is also true in half-apo PHM, then the Cu must be lost from the M-site and rebound at the H-site. Consistent with this idea, integration of both 2093 and 2062 cm^{-1} peaks in the presence of YVG provides a total area equal to that without bound YVG, suggesting that the total concentration of CO has remained constant. This also indicates that copper is not lost from half-apo but is redistributed between the two sites.

The question then arises: how does the substrate modulate the thermodynamic or kinetic stability of the copper centers? A partial explanation may lie in the observed magnitudes of the DW terms in the EXAFS simulations. Because the DW term for the Cu−S interactions is larger in half-apo than native enzyme, it is likely that the Cu−S bond is weaker, providing a mechanism for lowering of the K_m for copper binding in the Cu_M−carbonyl. Alternatively, it is possible that the peptide substrate may actively assist in the transfer of copper from Cu_M to Cu_H, perhaps via itself becoming a ligand to Cu_H in the substrate-activated carbonyl complex. This suggestion would explain the sensitivity of the 2062 cm^{-1} band to the structure of the peptide substrates.

In conclusion, half-apo PHM has unambiguously established binding of CO at the Cu_M center and has provided evidence that the chemistry at the active site of the native PHM is more complex than first thought. The possibility of an alternative peptide binding site perhaps involving ligation of peptide substrate to Cu_H is intriguing. Full characterization of the Cu_H site in the absence of Cu_M will be necessary to further substantiate these findings, and these experiments are underway.

ACKNOWLEDGMENTS

We thank Drs. Richard E. Mains and Betty E. Eipper for kindly providing us with cell lines as well as for many stimulating discussions on the expression, structure, and function of PHM. We gratefully acknowledge the use of facilities at the Stanford Synchrotron Radiation Laboratory (SSRL), which is supported by the National Institutes of Health Biomedical Research Technology Program, Division of Research Resources, and by the U.S. Department of Energy, Basic Energy Sciences (BES) and Office of Biological and Environmental Research (OBER).

SUPPORTING INFORMATION AVAILABLE

Tables of parameters (S1−S7) used to produce the best fits to the data given in Table 2. This material is available free of charge via the Internet at http://pubs.acs.org.

REFERENCES

1. Hazes, B., Magnus, K. A., Bonaventura, C., Bonaventura, J., Dauter, Z., Kalk, K. H., and Hol, W. G. J. (1993) *Protein Sci. 2*, 597−619.
2. Cuff, M. E., Miller, K. I., van Holde, K. E., and Hendrickson, W. A. (1998) *J. Mol. Biol. 278*, 855−870.
3. van Gastel, M., Bubacco, L., Groenen, E. J. J., Vijgenboom, E., and Canters, G. W. (2000) *FEBS Lett. 474*, 228−232.
4. Volbeda, A., and Hol, W. G. J. (1989) *J. Mol. Biol. 209*, 249−279.
5. Magnus, K. A., Hazes, B., Ton-That, H., Bonaventura, C., Bonaventura, J., and Hol, W. G. J. (1994) *Proteins 19*, 302−309.
6. Prigge, S. T., Mains, R. E., Eipper, B. A., and Amzel, L. M. (2000) *Cell. Mol. Life Sci. 57*, 1236−1259.
7. Klinman, J. P. (1996) *Chem. Rev. 96*, 2541−2561.
8. Prigge, S. T., Kolhekar, A. S., Eipper, B. A., Mains, R. E., and Amzel, L. M. (1997) *Science 278*, 1300−1305.
9. Prigge, S. T., Kolhekar, A. S., Eipper, B. A., Mains, R. E., and Amzel, L. M. (1999) *Nat. Struct. Biol. 6*, 976−983.
10. Blackburn, N. J., Hasnain, S. S., Pettingill, T. M., and Strange, R. W. (1991) *J. Biol. Chem. 266*, 23120−23127.
11. Blackburn, N. J., Rhames, F. C., Ralle, M., and Jaron, S. (2000) *J. Biol. Inorg. Chem. 5*, 341−353.
12. Francisco, W. A., Merkler, D. J., Blackburn, N. J., and Klinman, J. P. (1998) *Biochemistry 37*, 8244−8252.
13. Perkins, S. N., Husten, E. J., and Eipper, B. A. (1990) *Biochem. Biophys. Res. Commun. 171*, 926−932.
14. Bradbury, A. F., and Smyth, D. G. (1987) *Eur. J. Biochem. 169*, 579−584.
15. Merkler, D. J., and Young, S. D. (1991) *Arch. Biochem. Biophys. 289*, 192−196.

16. Tajima, M., Iida, T., Yoshida, S., Komatsu, K., Namba, R., Yanagi, M., Noguchi, M., and Okamoto, H. (1990) *J. Biol. Chem. 265*, 9602−9605.
17. Freeman, J. C., Villafranca, J. J., and Merkler, D. J. (1993) *J. Am. Chem. Soc. 115*, 4923−4924.
18. Merkler, D. J., Kulathila, R., Consalvo, A. P., Young, S. D., and Ash, D. E. (1992) *Biochemistry 31*, 7282−7288.
19. Noguchi, M., Seino, H., Kochi, H., Okamoto, H., Tanaka, T., and Hirama, M. (1992) *Biochem. J. 283*, 883−888.
20. Young, S. D., and Tamburini, P. P. (1989) *J. Am. Chem. Soc. 111*, 1933−1934.
21. Zabriskie, T. M., Cheng, H., and Vederas, J. C. (1991) *J. Chem. Soc., Chem. Commun.*, 571−572.
22. Reedy, B. J., and Blackburn, N. J. (1994) *J. Am. Chem. Soc. 116*, 1924−1931.
23. Boswell, J. S., Reedy, B. J., Kulathila, R., Merkler, D. J., and Blackburn, N. J. (1996) *Biochemistry 35*, 12241−12250.
24. Jaron, S., and Blackburn, N. J. (1999) *Biochemistry 38*, 15086−15096.
25. Nakamoto, K. (1986) *Infrared and Raman Spectra of Inorganic and Coordination Compounds*, 4th ed., John Wiley & Sons, New York.
26. Pasquali, M., and Floriani, C. (1984) in *Copper Coordination Chemistry: Biochemical and Inorganic Perspectives* (Karlin, K. D., and Zubieta, J., Eds.) pp 311−330, Adenine Press, Guilderland, NY.
27. Blackburn, N. J., Pettingill, T. M., Seagraves, K. S., and Shigeta, R. T. (1990) *J. Biol. Chem. 265*, 15383−15386.
28. Pettingill, T. M., Strange, R. W., and Blackburn, N. J. (1991) *J. Biol. Chem. 266*, 16996−17003.
29. Kolhekar, A. S., Keutman, H. T., Mains, R. E., Quon, A. S. W., and Eipper, B. A. (1997) *Biochemistry 36*, 10901−10909.
30. Eisses, J. F., Stasser, J. P., Ralle, M., Kaplan, J. H., and Blackburn, N. J. (2000) *Biochemistry 39*, 7337−7342.
31. Blackburn, N. J., Mason, H. S., and Knowles, P. F. (1980) *Biochem. Biophys. Res. Commun. 95*, 1275−1281.
32. Blackburn, N. J., Collison, D., Sutton, J., and Mabbs, F. E. (1984) *Biochem. J. 220*, 447−454.
33. Obata, A., Tanaka, H., and Kawazura, H. (1987) *Biochemistry 26*, 4962−4968.
34. Beltramini, M., Ricchelli, F., Piazzesi, A., Barel, A., and Salvato, B. (1984) *Biochem. J. 221*, 911−914.
35. Zolla, L., Calabrese, L., and Brunori, M. (1984) *Biochim. Biophys. Acta 788*, 206−213.
36. Eipper, B. A., Quon, A. S. W., Mains, R. E., Boswell, J. S., and Blackburn, N. J. (1995) *Biochemistry 34*, 2857−2865.
37. Sorrell, T. N., and Borovick, A. S. (1987) *J. Am. Chem. Soc. 109*, 4255−4260.
38. Fager, L. Y., and Alben, J. O. (1972) *Biochemistry 11*, 4786−4792.

BI002849Y